Colloids and Surfaces A: Physicochemical and Engineering Aspects 643 (2022) 128746

Contents lists available at ScienceDirect

Colloids and Surfaces A: Physicochemical and Engineering Aspects

journal homepage: www.elsevier.com/locate/colsurfa

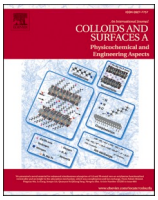

Effect of counter-ion on rheological properties of mixed surfactant solutions

Z. Mitrinova, H. Alexandrov, N. Denkov, S. Tcholakova *

Department of Chemical and Pharmaceutical Engineering, Faculty of Chemistry and Pharmacy, Sofia University, 1 James Bourchier Ave., 1164 Sofia, Bulgaria

GRAPHICAL ABSTRACT

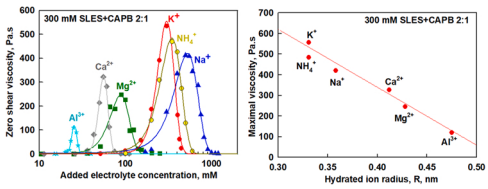

ARTICLE INFO

Keywords:
Electrolyte
Ion radius
Rheology
Micellar solutions

ABSTRACT

The effects of the charge, size and concentration of counter-ions (Na^+, NH_4^+, K^+, Mg^{2+}, Ca^{2+} and Al^{3+}) on the rheological properties of 300 mM SLES+CAPB surfactant solutions are studied and compared with results available in the literature for the effects of Na^+ and K^+ on SLES solution. The results show that all counter-ions studied are able to induce formation of wormlike micelles in a certain concentration range – as a consequence, the solution viscosity passes through a high maximum as a function of salt concentration. The salt concentration leading to maximum in the solution viscosity decreases with increasing the charge density of the counter-ion, defined as the ratio of the charge of the counterion and its hydrated radius, *Z/R*. The maximum viscosity in the salt curve decreases with increasing the hydrated radius of the counter-ion. The addition of CAPB to SLES leads to about 10-fold higher viscosity and to higher maximum viscosity in the presence of K^+ as compared to Na^+, whereas the opposite trend was observed for SLES alone. These effects are attributed to the interplay between the anionic and zwitterionic surfactants, and the electrolyte in the mixed SLES+CAPB system.

1. Introduction

Surfactant systems are widely used in different aspects of our life, like in personal and home care products. They possess peculiar behavior due to the ability of reversible aggregation into micelles which depends on the interactions between the molecules and their packing parameter [1,2]. The latter is governed by the balance of the hydrophobic and hydrophilic parts of the molecules. Smaller packing parameter corresponds to nearly spherical micelles due to the bigger head group, whereas bulkier hydrophobic tail leads to elongated micelles, vesicles, bilayers etc., see e.g. the different structures described by Israelachvili [2].

For diluted micellar systems with nearly spherical micelles, there is no overlapping between the aggregates, while the intermicellar interactions are very significant in the systems containing long wormlike micelles in the semi-dilute regime [3].

The effects of various factors on the micellar growth are widely studied in the literature. These studies showed that the aggregation changes are reflected in the rheological behavior of the surfactant solutions. The packing parameter could be manipulated by changing both the area of the hydrophilic head and the volume of the hydrophobic tail. The hydrophobic tail is mainly affected by the use of bulkier

* Correspondeing author.
E-mail address: sc@lcpe.uni-sofia.bg (S. Tcholakova).

https://doi.org/10.1016/j.colsurfa.2022.128746
Received 28 December 2021; Received in revised form 7 March 2022; Accepted 8 March 2022
Available online 11 March 2022

hydrophobic domains, e.g. in lipids possessing two chains per head [2]. On the other hand, the average volume of the chain could be modified by mixing components of different chain-lengths which, at appropriate balance, induces micellar growth [4–8].

Typically for ionic surfactants, the electrostatic interactions between the components in the micelles are changed by using binary mixture of oppositely charged surfactants which induces elongation of the micelles [9,10]. Another possibility is the addition of non-ionic surfactant with small head group which plays the role of a spacer and hinders the repulsion between the similarly charged head-groups [8,11–15]. The most widely used mode for formation of wormlike micelles (WLM) in ionic surfactant systems is the addition of counter-ions, which screen the electrostatic repulsion between the charged surfactant head-groups [1, 12,13,16–19]. The effect of electrolyte depends on both the ion charge and size. According to Hofmeister series [20,21] the ions could be ordered in a sequence, depending on their water affinity which allows one to predict the preferential interaction of oppositely charged ions in relation to their radius, charge or ion-charge density [22]. In general, the bare ions with smaller radius and higher charge possess higher charge density and behave as water structurants (kosmotropes) – they contain larger number of water molecules in their first hydration shell, thus leading to larger radius of the hydrated ion [22]. This larger size of the hydrated ions reduces their charge density and, thus, leads to weaker interaction with the ions of opposite charge present in the aqueous solution, including the surfactant ones.

The effect of the electrolyte type in diluted surfactant solutions has been studied extensively. Vlachy et al., 2009 [23] showed that the slope of the hydrodynamic radius increase vs. salt concentration depends on the interaction between the counterion and the anionic surfactant. These authors showed that Li^+ is less efficient as compared to Cs^+ in the case of dodecyl sulfate, whereas the opposite trend is observed with dodecyl carbonate. This trend was explained with the lower charge density of alkyl sulfonates as compared to alkyl carbonates. These authors classified the alkyl sulfate headgroup as chaotropic and the alkyl carboxylates – as kosmpotropes. Following the Collins's concept, they concluded that Cs^+ forms the closest ion pairs with dodecyl sulfate, whereas Li^+ forms the closest pair with dodecyl carboxylates. As a consequence, these ion pairs have smaller area-per-molecule (due to their reduced hydration) and higher packing parameter, thus facilitating the formation of bigger molecular aggregates as observed experimentally. The preferences for counter-ion interactions affect also the critical micellization concentration (CMC) [24–26]. Sharker et al. [26] showed that ions with larger hydrated radius interact weakly with sodium dodecylsulfate (SDS) and decrease to a lower extent the CMC of SDS, compared to the ions with smaller hydrated radius, such as K^+ and Cs^+. The chaotropic Cs^+ is the most effective in lowering the CMC of SDS while the strong kosmotrope Li^+ is the least effective.

Alargova et al., [27–30] studied the effect of mono, di- and trivalent ions on diluted SLES-2EO solution via dynamic and static light scattering, ultrafiltration and surface tension. They showed that the multivalent ions are much more efficient in inducing micelle elongation when compared to the monovalent ions. The effect of the different ions on SLES system is investigated also by small angle neutron scattering and neutron reflectivity [31]. Xu et al. [31] compared the effects of different trivalent ions on the surface properties and solution aggregation of SLES with 2 and 3 EO groups. They showed that the onset of both the formation of surface multilayer structures and micellar growth in solution depend on the nature of counterion and its hydration. For trivalent ions, the ion binding increases with the decrease of the hydrated ion size. Ions with smaller hydrated radius, such as Sc^{3+}, facilitate both the micellar growth in solution (before the formation of lamellar phases) and precipitation when compared to ions with larger hydrated radius, such as Al^{3+}. The later effect is attributed to the increased binding of Sc^{3+} compared to Al^{3+}, and the associated decrease in the hydration of the respective ion pair.

For more concentrated surfactant solutions, the effect of electrolyte could be quantified by studying the rheological behavior of the solutions. Qiao et al. [16] showed that for surfactant mixtures of SDS and tetradecyldimethylammoniumpropanesulfonate, the efficiency of counter ions in micellar growth decreases in the order $Al^{3+} > Ca^{2+}$, Mg^{2+}, $Zn^{2+} > Na^+$. Pleines et al. [1] studied the effect of monovalent counter ions added to anionic SLES. They showed that K^+ shifts the salt curve maximum to lower electrolyte concentrations when compared to Na^+ which is explained by the different dissociation constants of K^+LES^- and Na^+LES^- and by the opportunity of the K^+ ions to enter deeper in the hydrated shell of the micelle due to their smaller hydrated radius. In contrast, the more hydrated ions are less prompt to enter the hydration shell of the micelle and became less effective in screening the electrostatic interactions between the SLES molecules. Such effect was observed also for the cationic surfactant in the presence of different anions [18,19,32].

Although results for the effect of counter-ions with similar charge on the rheological properties of WLM solutions are available, as explained above, there is no systematic study about the effect of ions with different valence on the rheological salt curves of anionic-zwitterionic surfactant mixtures. Thus, we focused our study on the analysis of the effects of counter-ion charge and charge density on the rheological properties of concentrated surfactant solutions, aiming to generalize the effect of ionic parameters on the bulk rheological properties of SLES+CAPB surfactant mixtures.

2. Materials and methods

2.1. Materials

The solutions are prepared by mixing anionic surfactant sodium lauryl ether sulfate, SLES (product of Stepan Co., IL, USA; with commercial name STEOL CS-170 Stepan) and zwitterionic surfactant cocoamidopropyl betaine, CAPB (product of Goldschmith, with commercial name Tego Betaine F50). The effect of several electrolytes was investigated: sodium chloride (NaCl); potassium chloride (KCl); magnesium chloride hexahydrate ($MgCl_2.6H_2O$), products of Sigma Aldrich; calcium dichloride dihydrate ($CaCl_2.2H_2O$), product of Chem lab; aluminium trichloride hexahydrate ($AlCl_3.6H_2O$), product of Fluka.

A series of solutions containing studied electrolytes at varying salt (C_{el}) and constant surfactant (C_S) concentrations were prepared by adding salt solution to the surfactant mixture. Surfactant stock solution contained 15 wt% SLES+CAPB, at fixed 2:1 wt ratio, corresponding to ≈ 300 mM SLES and 150 mM CAPB (because the molar masses of SLES and CAPB are almost the same – 332 g/mol and 342 g/mol, respectively). Electrolyte stock solutions were also prepared at concentrations between 0.5 M and 4 M depending on the studied ion. Then concentrated surfactant solution was mixed with an electrolyte stock solution at room temperature and components were dissolved under mild stirring (at least 1 h) until clear homogeneous mixtures were formed. The working solutions contain 10 wt% total surfactant concentration (300 mM) and salt content between 3 mM and 1200 mM. The solutions were kept at room temperature for further studies and appear to be stable for several months after their preparation. Isotropic solutions without any lamellar phases and crystallites were obtained.

One should note that the mixed surfactant solution of SLES+CAPB (denoted as BS in the text) contains ≈ 112 mM NaCl for each 100 mM CAPB [14]. This admixture of NaCl originates from the CAPB synthesis and it is accounted for when considering the effect of the total electrolyte concentration or the ionic strength in the systems studied.

In Table 1 are summarized the molecular characteristics of the studied counter ions. The radii of hydrated ions are taken from the experimental data of conductivity measurements summarized in [2]. On the other hand, the thickness of the hydrated shell is calculated by the hypothetical volume of the water molecules in the first hydration shell around given ion at the assumption that they are part of a sphere, Marcus [33]. From [33] are taken also the standard molar Gibbs free

Table 1
Ionic radius [nm] for the cations of the studied salts, hydrated shell width [nm], number of water molecules in the hydrate shell, free Gibbs energy for ion hydration taken from Marcus [33]. Hydrated ion radius [nm] and ratio between charge and hydrated ion radius are calculated by using the data from Israelachvili [2].

Electrolyte	Ion	Bare ion	Hydrated ion				
		Ionic radius, nm	Hydrated ionic radius*, nm	Hydrated shell width, nm	Water molecules in hydrated shell	ΔG_{hydr}, kJ/mol	Z/R, nm^{-1}**
NaCl	Na^+	0.095	0.358	0.116	3.5	-365	2.8
KCl	K^+	0.133	0.331	0.074	2.6	-295	3.0
NH_4Cl	NH_4^+	0.148	0.331	0.065	2.4	-285	3.0
$MgCl_2$	Mg^{2+}	0.065	0.428	0.227	10.0	-1830	4.7
$CaCl_2$	Ca^{2+}	0.099	0.412	0.171	7.2	-1505	4.9
$AlCl_3$	Al^{3+}	0.050	0.475	0.324	20.4	-4525	6.3

energies of hydration for the studied ions. One can see from Table 1 that bigger bare ions have smaller hydrated radius and thus higher *Z/R* which means that their charge density is higher at otherwise similar charge. The ratio between ion charge and hydrated radius (*Z/R*) increases in the order $Na^+ < K^+ = NH_4^+ < Mg^{2+} < Ca^{2+} < Al^{3+}$. The difference between Na^+ and K^+ is relatively small while for the trivalent ion it increases up to 2.3 for Al^{3+} compared to Na^+.

2.2. Rheological properties

Rheological measurements were performed on rheometer Bohlin Gemini (Malvern Instruments, UK). Measurements were made by using cone and plate geometry with two different cone diameters depending on solution viscosity. For samples with low viscosity < 1 Pa.s, cone with diameter 60 mm and truncational angle 2° was used, and for those with viscosity above 1 Pa.s – cone was with diameter 40 mm and angle 4°.

The protocol for rheological measurements consists of 5 min thermal equilibration at 20 °C and then logarithmical variation of shear rate between 0.01 s^{-1} and 300 s^{-1}. The viscosity of each sample was determined by 2 independent measurements and the error was determined to be around 10%.

Oscillatory measurements were also performed at frequency sweep regime where applied frequency was varied between 0.01 and 10 Hz at 2% deformation, which correspond to the linear region in amplitude sweep experiment.

All rheological measurements were conducted at temperature of 20 °C.

2.3. SAXS measurements

SAXS measurements of the micellar solutions were carried out on an inhouse X-ray scattering system (XEUSS 3.0 SAXS/WAXS System, Xenocs, Sassenage, France) with a CuKα X-ray source (λ = 0.154 nm, Xeuss 3.0 UHR Dual source Mo/Cu, Xenocs, Sassenage, France) and Eiger2 4 M detector (Dectris Ltd., Baden Deattwil, Switzerland) with slit collimation. The apparatus was operated at 50 kV and 0.6 mA. The sample to detector distance (SDD) of 1000 mm and 3000 mm allowed to access the Q-range of 0.01–0.5 $Å^{-1}$. Data acquisition time was 30 min. Samples were enclosed into vacuum tight thin borosilicate capillary with an outer diameter of 1 mm and thickness of 10 μm. The scattered intensity was normalized to the incident intensity, and were corrected for the background scattering from the capillary. It was calibrated to absolute scale. The measurements were performed at ambient temperature 20 °C. For the SAXS data modelling the software SASView was used.

3. Experimental results

All prepared samples appear transparent in the studied concentration range. The threshold concentrations for the phase separation are shown in Table S1. The lowest threshold concentration was for $AlCl_3$ (42.5 mM), whereas the solutions remain transparent even at 1200 mM NaCl. This indicates, as expected, that multivalent ions are much more efficient in formation of neutral ion pairs with SLES molecules which leads to precipitation and phase separation. This phase separation could be attributed to predominance of junction formation [34].

Fig. S1 shows typical rheological behavior of the studied systems from which the viscosity parameters are determined. Samples with the lowest electrolyte concentration have nearly Newtonian behavior and their viscosity slightly depends on the shear rate. Gradually, with the increase of the salt content, the rheological behavior switches to non-Newtonian shear thinning, characterized with a plateau in viscosity at low shear rates and then gradual decrease with the increase of the shear rate. This behavior is typical for wormlike micellar solutions which are visco-elastic and show Maxwellian relaxation. The shear thinning behavior above the critical shear rate is usually described as $\eta \propto 1/\dot{\gamma}$ and it is often taken as an evidence of the presence of wormlike micelles that undergo a structural change under shear, such as the alignment of the long micelles at high shear rates or shear banding [35–37]. The presence of WLM is confirmed by the measurements in the oscillatory regime showing a visco-elastic behavior and described well by a "Cole-Cole" plot, see Supplementary Figs. S2 and S3.

For the samples of low viscosity with nearly Newtonian behavior, the viscosity was determined by Newton's law. For systems with shear-thinning behavior the low-shear viscosity was taken from the plateau region. All determined viscosities were used for plotting the salt curves, viz. the dependence of viscosity on electrolyte concentration. Salt curves are usually used to describe the effect of electrolyte concentration on micellar solutions viscosity [1,13,17–19]. It could be explained as follows: at low electrolyte concentration the mixed micelles have nearly spherical or ellipsoidal shape [38], which is governed by the interactions between the anionic SLES and zwitterionic CAPB molecules. The increase of the salt content, corresponding to increase in the counter-ion concentration, screens the electrostatic repulsion between the similarly charged SLES molecules in the micelles, thus decreasing the mean area per molecule and leading to higher packing parameter. At higher ion concentration, near to the viscosity maximum, the micellar aggregation number increases dramatically and wormlike micelles are formed which form entangled structure. At the right-hand side of the maximum, viscosity decreases mainly due to formation of branched micelles [10, 39,40].

In Fig. 1 we compare the salt curves for all studied ions. The curves for samples containing NaCl are on the right, meaning that higher salt concentration is needed to induce WLM formation. In contrast, the peak for $AlCl_3$ is reached at the lowest added concentration. The required concentration for reaching viscosity maximum in the salt curves is decreasing in the order $Na^+ > NH_4^+ \sim K^+ > Mg^{2+} > Ca^{2+} > Al^{3+}$. This in fact is the same order in which *Z/R* ratio increases, see Table 1 which shows that the highly charged ions are more efficient in screening electrostatic repulsion between SLES head groups and decreasing the area per molecule at lower salt level as compared to other ions. The obtained results for lower required concentration to induce micelle growth in presence of multivalent ions for SLES+CAPB system are in good agreement with results reported in the literature for increased hydrodynamic radius of SLES micelles after addition of multivalent ions [27,29,30]. The results are also in good agreements with results reported by Missels et al. [41] where it was shown that for monovalent ions, the decrease in

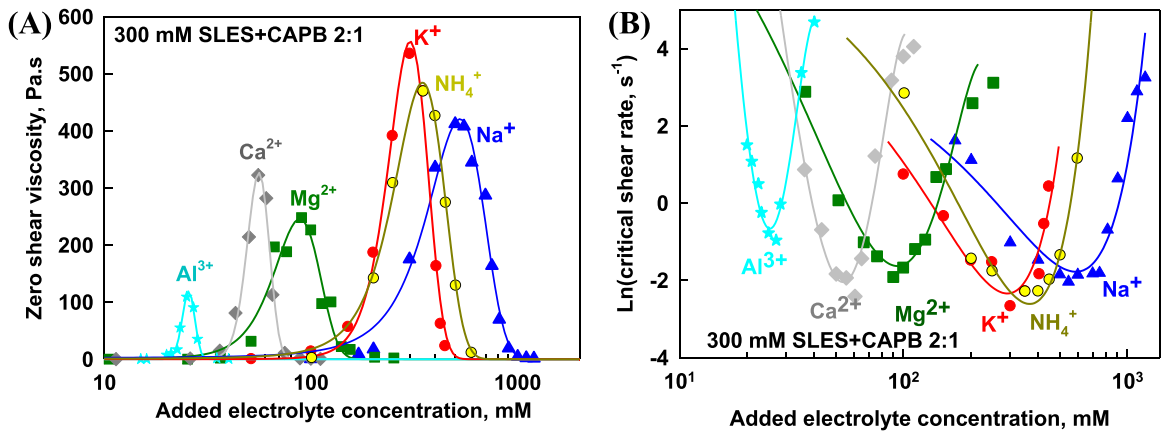

Fig. 1. (A) Zero shear viscosity as a function of added electrolyte concentration; (B) Critical shear rate as a function of added electrolyte concentration.

hydrated radius of the counter ion leads to higher degree of micellar growth for dodecyl sulfate surfactant, meaning that the more hydrated ions give smaller micelles at low salt concentrations.

One can see from the rheological curves (Fig. S1) that they are shifted not only with respect to the different viscosity depending on the electrolyte concentration, but also the plateau region at low shear rates is extended to the different shear rates. From these curves the critical shear rate could be determined, corresponding to the point at which the viscosity starts to decrease and shows shear-thinning behavior. As long as viscosity passes through a maximum at intermediate salt concentrations, the critical shear rate passes through a minimum. From this presentation the electrolyte concentration for the minimum position in curves was determined, see Fig. 1B.

One should mention that CAPB also contains certain amount of NaCl as an admixture. That is why in the studied systems the counter ion concentration is coming not only from the added electrolyte but also from the zwitterionic surfactant. The anionic surfactant SLES added to the aqueous solution undergoes dissociation, characterized by the dissociation constant k_d:

$$k_d = \frac{[Na^+][LES^-]}{[Na^+LES^-]} \quad (1)$$

Similar expressions can be written for all other counterions present in the solutions. It was shown in Ref. [1] that k_d for NaLES is 0.26 M and for KLES it is 0.11 M, which implies that K^+ is bound stronger to LES^- as compared to Na^+. By using the value of k_d for NaLES it can be estimated that the degree of SLES ionization in solutions varies between 1 and 0.2, depending on NaCl concentration. The latter value is in a good agreement with the results reported in Ref. [42]. In the presence of KCl, accounting for the presence of Na^+ coming from the original SLES, one can calculate that the SLES ionization decreases down to 13%. In other words, there are sodium cations and alkylether sulfate anions in the aqueous solution, but also non-dissociated SLES molecules.

In the total ion concentration of the studied samples one should account for each ion with its charge contribution to the ionic strength of the solutions. The latter is defined as follows:

$$I = \frac{1}{2}\sum_{i=1}^{n}(c_i Z_i^2) \quad (2)$$

where c_i is a concentration of a given ion and Z_i is an ion charge. It is worth plotting the salt curves as a function of ionic strength coming from the cations which will affect the anionic surfactant and the total ionic strength in order to account for the charge contributions.

In Fig. 2 are shown salt curves as a function of ionic strength coming from cations only or from all present ions. In both cases the values are calculated with summation of the added salt, salt from CAPB, and sodium ions from SLES molecules, accounting for the full surfactant dissociation. In all cases, the highest ionic strength for induction of the micellar growth is required for Na^+, while for Ca^{2+} and Al^{3+} is the lowest. For the total ionic strength, we see that the peak position is similar for Mg^{2+} and K^+, as it is for Ca^{2+} and Al^{3+}, whereas the peak position for Mg^{2+} is closer to that of NH_4^+ when considering the ionic strength coming from the cations only.

The micellar growth depends on the packing parameter which on its own is governed by the area per molecule. The head group area changes, depending of the degree of neutralization of the surfactant molecules surface charges. In Fig. 3 are shown the results for viscosity as a function

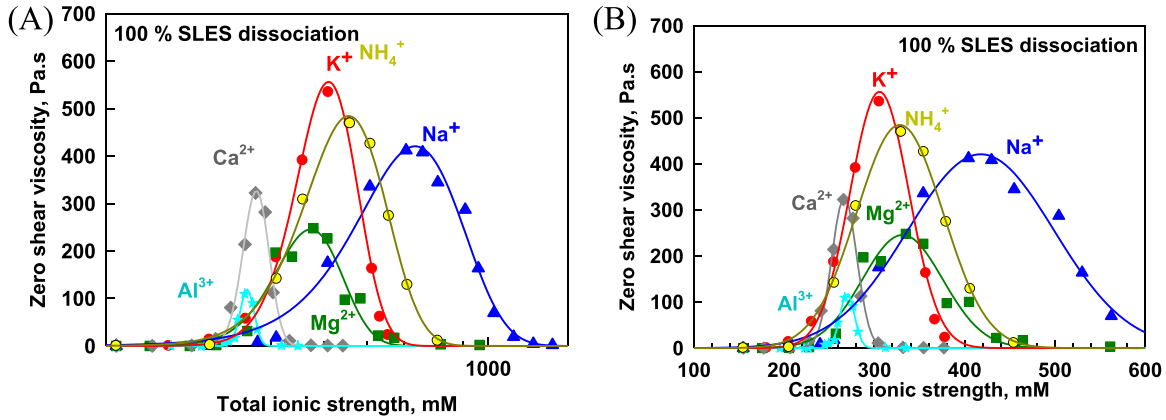

Fig. 2. Viscosity as a function of (A) total ionic strength and (C) ionic strength coming from the cations. The curves are showing the results under the assumption of 100% dissociation of SLES molecules.

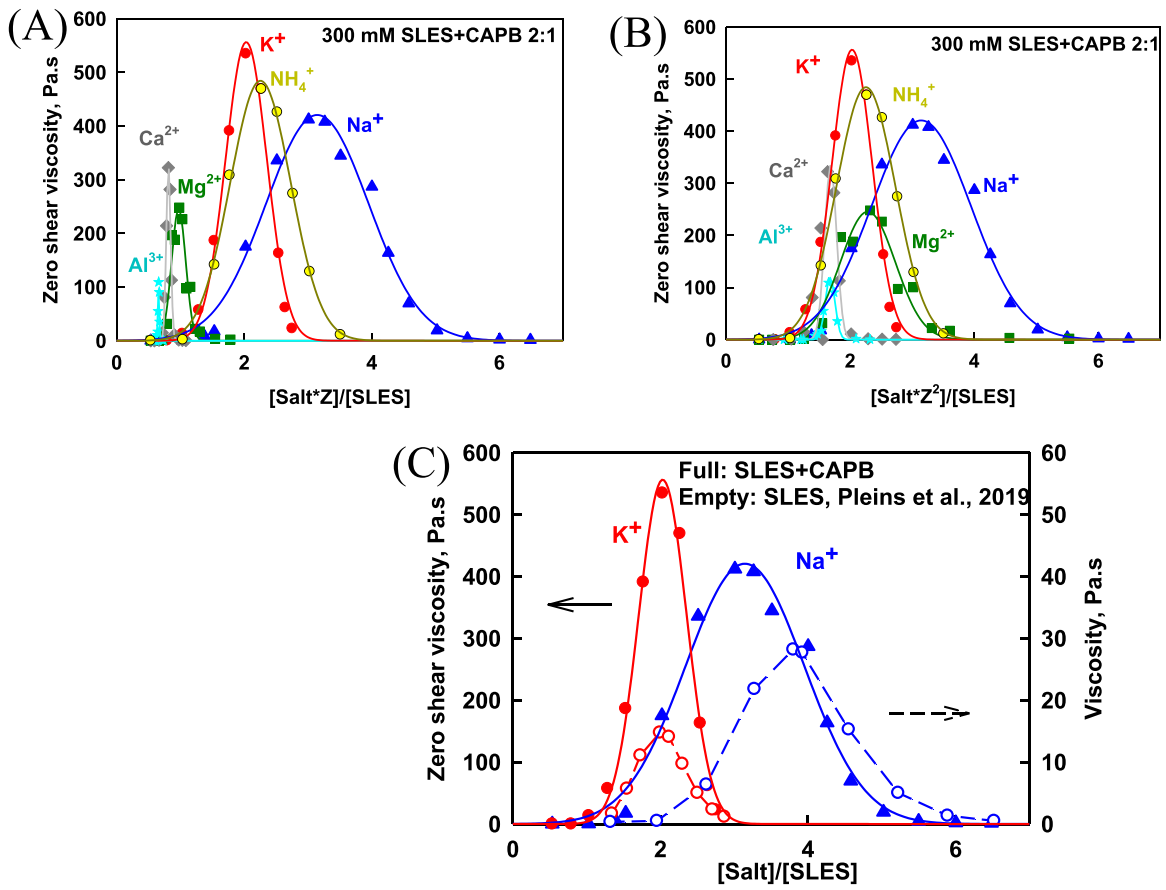

Fig. 3. Viscosity as a function of counter ion to surfactant ratio accounting for the effect of ion charge on (A) first power or (B) second power. (C) Comparison between the results for SLES from Pleines at al. [1] and SLES+CAPB from current study.

of C_{el} to SLES concentration ratio. This ratio could be attributed to the degree of the micelle's complexation as long as the total surfactant concentration is well above CMC, which for SLES+CAPB= 2:1 is≈ 0.5 mM, while the total surfactant concentration is 200 mM for SLES [43].

One can see that for Na^+ the viscosity peak is reached at the highest counter-ion to SLES concentration ≈ 3.1, while K^+ induces WLM formation at lower ion to surfactant ratio of 2.0 compared to Na^+. These trends are in good agreement with results reported by Pleines et al. [1] who showed that for SLES alone (without CAPB) counter ion/LES^- ratio is 3.75 for Na^+ and 2.0 for K^+, see Fig. 3C. On the other hand, Ca^{2+} and Al^{3+} induce viscosity peak formation at the lowest counter-ion to surfactant ratio of ≈ 1.7. This shows much stronger interaction between surfactant and Ca^{2+} compared to the other di-valent ion Mg^{2+}. In addition, for Na^+ the peak is the broadest and for Ca^{2+} and Al^{3+} it is the narrowest.

In Table 2 we summarize the values for the viscosity at the peak and the salt concentration corresponding to this point. One sees that the viscosity at the maximum is the highest for K^+ as compared to Na^+. Similar trend is determined for Ca^{2+} and Mg^{2+}. Therefore for SLES+CAPB mixture not only the amount of required salt is lower when the bare ion size is bigger but also the viscosity that is reached is higher. These effects imply that the presence of CAPB in the mixture not only increases the viscosity of the mixture by 10 times as can be seen from Fig. 3C, but also changes the effect of the bare ion size on the viscosity maximum.

The experimental data from oscillatory experiments for systems with salt concentrations around the maximum in their salt curves are shown in Figs. S2 and S3. These results are analysed to obtain the information for the relaxation, breakage and reptation times of the micelles, the mesh size of the micellar network, and the number of entanglements per micelle. The equations used for extracting this information are described in Ref. [8] and the obtained results are summarized in Table 3. The mesh size of the micellar network depends slightly on the counterion type – it varies between 30 nm for Na^+ and 36 nm for Al^{3+}. Note that similar mesh size was determined from rheological measurements of

Table 2
Comparison between the critical shear rate at the minimum, viscosity in the salt curve maximum, added salt concentration at the maximum, ration between ionic ionic strength from the cations and SLES concentration, ionic strength coming from cations and the total ionic strength of the solution (the concentration of LES^- is excluded).

Ion	Critical shear rate at minimum, s^{-1}	Viscosity at maximum, Pa.s	Concentration at viscosity maximum, mM	[Salt]/[SLES]	Ionic strength coming from cations, mM	Total ionic strength at maximum, mM
Na^+	0.2	420.6	526.5	2.09	418.0	735.2
K^+	0.1	556.5	301.8	1.53	305.6	510.5
NH_4^+	0.1	484.4	346.9	1.64	328.2	555.6
Mg^{2+}	0.2	245.6	88.2	1.66	331.2	473.4
Ca^{2+}	0.4	326.7	56.0	1.33	266.7	376.6
Al^{3+}	0.8	119.0	25.6	1.35	269.9	362.3

Table 3
Values of the zero-shear viscosity, η_0, characteristic frequency, ω_C, relaxation time, τ_R, plateau modulus, G_0, mesh size of the micelle network, ξ, minimum in the viscous modulus as a function of frequency, $G_m``$, number of entanglement points per micelle, n_{ent}, micelle breakage time, τ_{br}, and micelle reptation time, τ_{rep}, for the various chemical classes of cosurfactants. The data, corresponding to a maximum in the values of η_0 for a given class of cosurfactant, are shown in bold. The abbreviation BS indicates 300 mM SLES+CAPB solution in 2:1 ratio.

System	η_0, Pa.s	ω_C, rad/s	τ_R, s	G_0, Pa	ξ, nm	G''_{min}, Pa	n_{ent}	τ_{BR}, s	τ_{REP}, s
BS+550 mM NaCl	408	0.27	3.7	147	30.2	5.3	28	1.4	9.7
BS+350 mM NH_4Cl	469	0.22	4.5	123	32.0	5.0	24	1.7	11.9
BS+300 mM KCl	534	0.19	5.2	126	31.7	5.3	23	2.0	13.7
BS+90 mM $MgCl_2$	248	0.55	1.8	133	31.2	7.2	18	0.7	4.8
BS+55 mM $CaCl_2$	322	0.34	3.0	108	33.5	7.1	15	1.1	7.9
BS+25 mM $AlCl_3$	111	0.77	1.3	87	36.0	10.6	8	0.5	3.4

SLES+CAPB solutions in the presence of various additives in our previous study [8]. For all systems studied, the reptation time is longer as compared to the breakage time which means that these systems are in the so-called "fast breakage regime", in which several scission and recombination events occur within the reptation time scale [13]. The breakage, reptation and relaxation times decrease in the following order: $K^+ > NH_4^+ > Na^+ > Ca^{2+} > Mg^{2+} > Al^{3+}$, thus indicating that longer micelles are formed with monovalent ions, as compared to divalent and trivalent ions. The number of entanglement points per micelle is also larger for monovalent as compared to divalent and trivalent ions. For ions with the same charge, the number of entanglements is higher for larger hydrated ions.

Additional experiments with SAXS were performed to investigate the micellar structure near the viscosity peak. To get the entire structure of WLM one needs USAXS/USANS, due to the presence of micrometer sized objects which are beyond the scope of this technique. Nevertheless, the SAXS measurements were performed which covered the size range of 1–100 nm. The samples were chosen near the viscosity peak for a given salt curve and the scattering data are shifted by factor of 3 for better illustration, see Fig. 4. All studied samples have similar profile in the high q-region with a broad peak which is typical for micellar solutions and corresponds to the distance between the surfactant head groups [44]. The minimum before the peak is correlated with the radius of the objects [45,46] and the shift leftwards in the presence of electrolytes is an indication for micellar growth. The main difference in the scattering pattern is in the low q-region which corresponds to bigger objects, following the relation $d = 2\pi/q$. Usually the power law dependence of $I(q)$ vs. q determines the type of structures: 0 for spheres, − 1 for cylinders and so on [47,48]. In our case, the power law index is the lowest for BS ≈ 0.4 which means that the micelles are not spherical. For all other systems, this coefficient is close to unity implying presence of cylindrical objects, see Table 4.

It is known that SLES+CAPB mixture in presence of salts is described well by a core-shell cylinder model [49,50] which is appropriate for micellar solutions. Here, the mixtures in the presence of different salts

Table 4
Results from the analysis of SAXS data. The cylinder core radius, R_C, cylinder shell thickness, t_{shell}, and cylinder shell scattering length density, ρ_{shell}, as determined from the best fit to the experimental data from SAXS measurements $I(q)$ for q between 0.03 and 0.3 $Å^{-1}$ using the model of infinitely long core-shell cylinders (L=720 nm was set). The total radius R_{tot} is the sum of $R_C + t_{shell}$. The values of solvent scattering length density $\rho_{SOL} = 9.44 \times 10^{-6}$ $Å^{-2}$ (calculated under the assumption that the solvent is pure water) and the cylinder core scattering length density $\rho_C = 7.32 \times 10^{-6}$ $Å^{-2}$ (calculated under the assumption that the micelle core has the scattering length density of dodecane) are used to perform the data fits. The abbreviation BS indicates 300 mM SLES+CAPB solution in 2:1 ratio.

System	Scale factor	ρ_{shell}, 10^{-6} $Å^{-2}$	R_{core}, nm	t_{shell}, nm	R_{tot}, nm	Slope in low q range
BS						-0.4
+350 mM KCl	1.3	9.526	0.577	2.835	3.412	-0.7
+550 mM NaCl	1.0	9.525	0.538	2.792	3.330	-0.9
+350 mM NH_4Cl	0.91	9.527	0.571	2.780	3.351	-1.1
+90 mM $MgCl_2$	0.36	9.603	0.702	2.623	3.325	-0.8
+55 mM $CaCl_2$	0.19	9.629	0.738	2.537	3.275	-0.5
+25 mM $AlCl_3$	0.11	9.673	0.822	2.401	3.223	-0.7

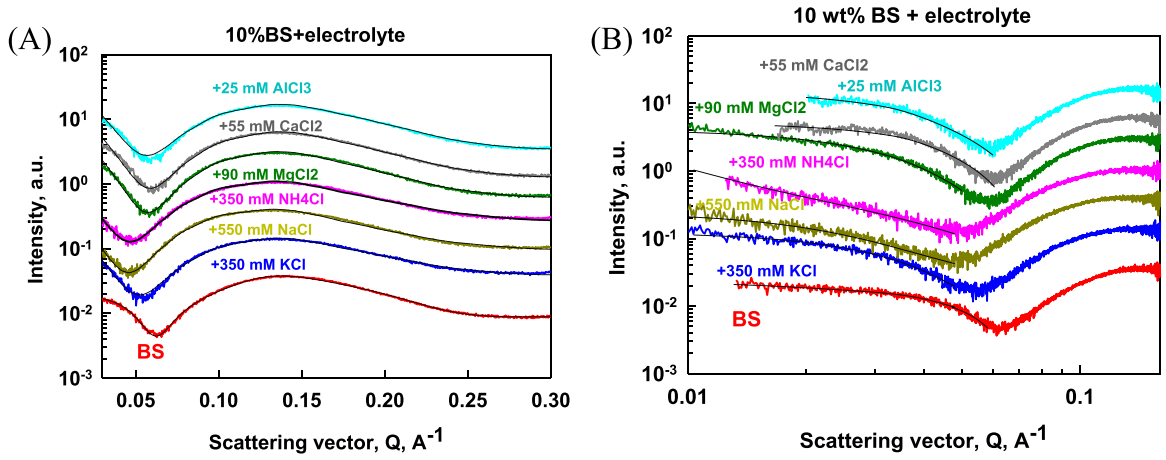

Fig. 4. Scattering curves measured at (A) 1000 mm and (B) 3000 mm sample to detector distance. Samples are denoted as follows: BS (red); + 350 mM KCl (blue); + 90 mM $MgCl_2$ (green); + 550 mM NaCl (yellow); + 350 mM NH_4Cl (pink); + 55 mM $CaCl_2$ (grey) and + 25 mM $AlCl_3$. Black solid lines denoted fitted curves via (A) core-shell ellipsoid model and (B) flexible cylinder. (For interpretation of the references to color in this figure legend, the reader is referred to the web version of this article.)

are evaluated through such analysis. The data evaluation was made by using SASView software (http://www.sasview.org). The results in the higher q region are fitted with core-shell cylinder model with infinity large length, see the black solid curves in Fig. 4. For BS system, the ionic interactions between the micelles are accounted by using the Hayter-Penfold approximation. For this system, the salt concentration is moderate. On the other side, all samples containing electrolyte of high concentration are described by infinity cylinders without accounting for the intermicellar interactions which is due to the screened electrostatic interactions at these concentrations, causing the micellar growth. The fitting parameters are shown in Table 4.

In the low q range the curves were analysed for WLM. This type of micelles was already identified by the samples rheological behavior including transparent solutions with shear thinning viscoelastic behavior described by Maxwellian relaxation mode. Typically, wormlike micelles are well fitted with the model for flexible cylinders [45, 52–54] [51] and here are shown the fits with black solid curves in Fig. 4B. Only the BS solution is fitted by a cylinder model.

The extracted data from the analysis of SAXS spectra in the q-range between 0.03 and 0.3 $Å^{-1}$ are shown in Table 4. One sees that the total micelle radius is $\approx 3.3 \pm 0.1$ nm for studied systems, which is in a good agreement with the results reported in Ref. [50] for SLES:CAPB at 3:5 ratio. For our systems, we found that the data can be fitted adequately only if account is taken for the different radii of the core and the shell thicknesses of the micelles, whereas in Ref. [50] the radius of the core and shell thickness were fixed to be the same for all systems studied. One probable reason for this difference in the data interpretation could be the higher surfactant concentration in the current study. The extracted parameters show that the shell thickness is the largest for monovalent ions, intermediate for Mg^{2+} and the smallest for Al^{3+} and Ca^{2+}. These results show that the water molecules penetrate deeper into the micelle core for Na^+ containing system as compared to K^+ and NH_4^+. The deeper penetration of water molecules is observed also for the system containing Mg^{2+} as compared to Ca^{2+}.

4. Discussion

The maximal viscosity for a given salt curve corresponds to the solution with the longest WLM, because the viscosity depends strongly on micellar length, L: $\eta \propto L^3$ [55]. It is expected that the mean number of entanglements between the micelles is the highest around the salt curve maximum, because this number is proportional to the micellar length $n_{ent} \propto L$ [55]. In other words, the highest viscosity corresponds to the longest micelles with the highest number of entanglements.

Note that we use in our study two groups of ions (Na^+, K^+ and NH_4^+) and (Mg^{2+} and Ca^{2+}) which have similar valence but differ in their hydrated ion radius and Z/R ratio, Table 1 . As explained, hydrated Na^+ ion has larger radius and lower charge density compared to the hydrated K^+, which leads to lower dissociation constant and higher charge neutralization ability of K^+ as compared to Na^+. Thus, lower K^+ concentration is sufficient to reach the packing parameter corresponding to WLM formation, see Fig. 1. Similar effect for the pair Na^+ and K^+ was observed for SLES [1], which showed that the salt curve for K^+ is shifted leftwards due to the stronger interaction with SLES. Comparing the bivalent ions Ca^{2+} and Mg^{2+} we see that Ca^{2+} has higher Z/R ratio and is more effective in micellar growth than Mg^{2+} – the same trend as observed with the monovalent ions. The stronger effect of Ca^{2+} compared to Mg^{2+} is also related to the lower dissociation constant of Ca^{2+} to SLES molecules as compared to Mg^{2+} (stronger interaction between Ca^{2+} and sulfate group).

From all studied ions, the three-valent Al^{3+} is the most efficient for inducing viscosity increase (it occurs at the lowest salt concentration compared to the other ions) but also the maximum in the salt curve is of the smallest amplitude. These trends imply that the dissociation constant of Al^{3+} with SLES is the lowest, however, the formed micelles are not so long and the number of entanglements is smaller when compared with Na^+ as can be seen from Table 3 above. Apparently, the Al^{3+} ions facilitate the micelle branching, thus relaxing the stress upon shear.

Comparing the maximum value of the viscosity in the salt curves, one can see that it depends strongly on the counterion added, which is related to the different interactions between the SLES and CAPB molecules and the various counterions. In Fig. 3C one sees that K^+ leads to higher maximum viscosity in the salt curves compared to Na^+ which is contrary to the results by Pleines et al. [1] who showed that K^+ ions decrease the salt curve amplitude compared to Na^+ for solutions of SLES only. The authors explained this effect with the larger penetrating ability of K^+ into the hydrated layer at the micelle-solution boundary which decreases the bending constant and increases micelle flexibility [1] because lower bending modulus corresponds to smaller persistence length. Oelschlaeger et al. [19] also showed that lower amplitude of salt curve for CTAB is observed with addition of less hydrated anions, but they mentioned that the penetrating hydrotrope (NaSal), added to CPyCl leads to higher viscosity at the salt curve maximum. One should mention that in both studies a single surfactant system was analyzed in the presence of electrolytes. In contrast, our system is a surfactant mixture which changes the electrostatic interactions and the packing parameter when compared to the single surfactant system [38].

Fraction of the sulfate groups in the SLES+CAPB mixture are already neutralized by the positive charges in the CAPB molecules, while the remaining COO^- charges in the CAPB molecules have higher affinity to Na^+ as compared to K^+. Indeed, as shown by Vrbka et al. [56] the Na^+/K^+ ratio in the vicinity of acetate anion is 3.4. The affinity of Na^+ ions to carboxylate groups was studied also by Vlachy et al. [23] who showed that the free energy change upon replacing potassium with sodium ion pair of acetate and methylsulfate ions is negative for acetate and positive for methylsulfate ion, thus showing that Na^+ ions prefer strongly the acetate ions, whereas K^+ ions prefer the methylsulfate ions. Therefore, K^+ penetrates deeper into the palisade layer of SLES, while Na^+ has higher affinity for the carboxyl groups of the CAPB molecules.

When analysing the viscosity curves, one should consider also the different structures of the palisade layers of the SLES and SLES+CAPB mixed micelles as illustrated in Fig. 5. One sees from Fig. 3C that the viscosities at the maximum of the salt curves are around an order of magnitude higher for the mixed SLES+CAPB system when compared to SLES alone. This is due to the predominant repulsion between the surfactant molecules in the SLES system, in contrast to the tighter packing of the two components in the mixed SLES+CAPB micelles, promoted by the alignment of the negative sulfate group in SLES close to the positive N-atom from the betaine headgroup in CAPB [38]. As a result, even without added electrolyte, there is a partial screening of the repulsion between the sulfate groups of SLES by the positive charges at the N-atom in CAPB.

Combining the information from the various experiments, we could propose the following mechanistic explanations of the observed effects of the various ions on the SLES and SLES+CAPB micelles, see Fig. 5. The maximum of the salt curves is explained with the transition from entangled to branched elongated micelles, Fig. 5 A,B. Therefore, the counterions which bind stronger to the surface head-groups (viz. those with lower k_d) would shift the onset of the viscosity increase towards the left. On the other hand, the position and the magnitude of the peak in the salt curves depend on the transition from the entangled into branched micelles which appears to be strongly affected by the ion type. To analyse this transition, we should account for the fact that the cylindrical body of the micelles has a radius of curvature, R_{tot}, which is similar in all these systems. In the branched micelles, however, we have local saddle-shaped surfaces at the branching points which have an additional radius of curvature of opposite sign, $-R_{br}$. Note that by convention the convex surfaces have positive radius of curvature, whereas the concave surfaces have negative radius of curvature. Therefore, the transition from entangled into branched micelles depends strongly on the energy penalty upon the formation of the saddle-shaped surface, viz. on the magnitude of the bending modulus, k_{bend} [1]. As

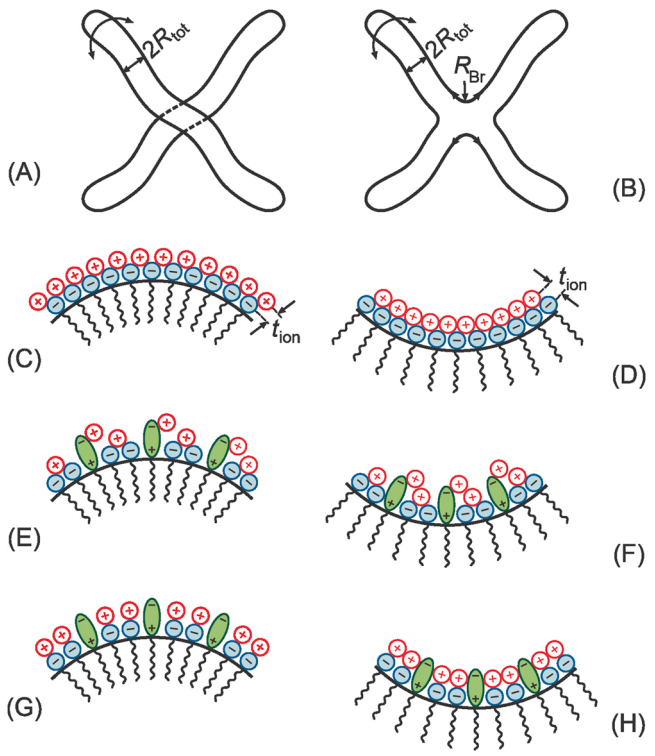

Fig. 5. Schematic presentation of (A) two entangled WLM and (B) branched micelles with the respective radii of curvature: R_{tot} for the cylindrical body of the micelles in both cases and the additional $-R_{br}$ in the branching region which has a saddle-shaped surface; note the opposite signs of R_{tot} and $-R_{br}$. (C, D) Schematic presentation of the counterion contraction when transforming the convex surface of the cylindrical SLES micelle into saddle-shaped surface at fixed area-per-molecule; note that this contraction is more extensive for bigger hydrated counterions (larger thickness of Stern layer, t_{ion}). In other words, the bending stiffness is larger for the bigger hydrated ions and it is more difficult to create branched micelles with them. This picture implies that for SLES micelles and ions of the same valence the following sequence holds: $R_{ion}\uparrow \Rightarrow t_{ion}\uparrow \Rightarrow k_{bend}\uparrow \Rightarrow \eta_{max}\uparrow$. (E–H) Schematic presentation of the transformation of the convex surface of the cylindrical SLES+CAPB micelles into saddle-shaped surface; note that the counterions here are distributed in space to neutralize both the sulfate heads of SLES and the carboxylate heads of CAPB. The experiments show that the addition of CAPB to SLES leads to an order of magnitude higher viscosity at the maximum of the salt curves which is due to the tighter packing of the SLES and CAPB molecules in the micelles. Here the bending is easier for the counterions which bind stronger to the carboxylate groups and neutralize them completely, viz. for Na^+ (E,F) as compared to K^+ (G,H). In other words, the smaller hydrated ions (e.g. K^+) bind preferentially to the sulfate groups next to the micelle surface and the surface bending is hindered because the carboxylate groups in CAPB repel electrostatically each other, suppressing the formation of branched micelles. This picture implies that for SLES+CAPB micelles and ions of the same valence, the sequence is the following: $R_{ion}\uparrow \Rightarrow k_d(COO^-)\uparrow \Rightarrow k_{bend}\downarrow \Rightarrow \eta_{max}\downarrow$.

shown in Fig. 5C,D, the formation of the saddle-shaped surface in the case of SLES micelles is related to contraction of the counterions in the Stern layer (expected to be electrically neutral under these conditions) which is more extensive for the bigger hydrated counterions, R_{ion}. In other words, for SLES micelles and ions of the same valence, the following sequence is expected to hold: $R_{ion}\uparrow \Rightarrow k_{bend}\uparrow \Rightarrow \eta_{max}\uparrow$. In contrast, the counterions on the surface of the mixed SLES+CAPB micelles are distributed in space to neutralize both the sulfate heads of SLES and the carboxylate heads of CAPB, Fig. 5E–H. Note that Na^+ and K^+ ions have different binding affinity to the sulfate and carboxylate groups. Here the bending is easier for the counterions which bind stronger to the carboxylate groups and neutralize them completely, viz. for Na^+ when compared to K^+. In other words, for SLES+CAPB micelles and ions of the same valence, the sequence is the following: $R_{ion}\uparrow \Rightarrow k_{bend}\downarrow \Rightarrow \eta_{max}\downarrow$.

One sees that the counterion charge and radius are crucial for the surfactant rheological properties. The dependence of the maximum viscosity of the SLES+CAPB mixtures on the hydrated ion radius is illustrated in Fig. 6. The maximum viscosity decreases linearly with the increase of the ion hydrated radius, the counterion charge being of no importance for this quantity. Note that the relaxation, breakage and reptation times also correlate very well with the size of hydrated ions – the ions with bigger hydrated radius have shorter breakage time of the micelles and higher stress relief, as compared to the ions with smaller hydrated radius. For bigger hydrated ions, e.g. Al^{3+}, the equilibrium is shifted to branched micelles instead of entangled WLM, which results in decrease of the maximum solution viscosity in the salt curve. This means that it is easier to form branched micelles in the Al^{3+} containing systems.

The increase of Z/R ratio leads to stronger interaction with the ionic surfactant and thus changes the position of the salt curve to lower concentrations. This position is expected to depend mainly on the dissociation constant of SLES-counterion pair, as shown in the work of Pleines et al. [1]. To account for the effect of the counterion charge, we plot in Fig. 6B the added electrolyte concentration for reaching the viscosity maximum, as a function of the charge/radius ratio for a given ion. The observed dependence is of a power-law type, with a power-law index of −3.4. This trend shows that the higher interaction energy between the surfactant anion and the counterion leads to lower electrolyte concentration for reaching a packing parameter corresponding to WLM formation. Considering the equally charged ions, this dependence shows that the hydrated counterions with smaller radius have stronger electrostatic interaction with the surfactant anions – these ions get closer to the micelle surface. The consequence is a lower surface charge density of the micelles, lower area-per-molecule and higher packing parameter, reached at lower electrolyte concentrations.

As proposed in the Collins' model for ions affinity [22], small and hard cations interact preferentially with small and hard anions (viz. ions with similar water affinity interact stronger). This is due to their ability to lose water molecules from their hydration shell, thus forming direct contact pairs which leads to free energy gain due to increase in the entropy of the released water molecules. In our case, alkyl polyoxyethelene sulphate group in SLES is of chaotrope type while the carboxylate group in CAPB is of kosmotrope type [57]. Therefore, it is unclear in advance whether the preferential interactions will be with Na^+ or K^+ counterions in such mixed surfactant system. We see from the experiments that the concentrations required to increase the viscosity of the solution increase in the order $K^+ < NH_4^+ < Na^+$ without following the direct or the reverse Hofmeister series. Note that according to Ref. [57] the Hofmeister order of counterions is $NH_4^+ > K^+ > Na^+$.

One additional aspect of the effect of ions is the critical shear rate/stress at which the shear thinning appears. This phenomenon is typical for wormlike micellar solution and it is attributed to the flow instability in a given range of shear rates. Spenley et al. [35] showed that the critical shear rate is related to the relaxation time and plateau modulus by the expressions: $\tau_{cr} \sim G_0$ and $\gamma_{cr} \sim T_R^{-1}$. This means that the systems with higher critical shear rate possess faster relaxation process. One can see from the data shown in Table 3 that the order of decrease of the relaxation times is the same as the order of increase of the hydrated ion radius, thus implying that the bigger ions are unable to stabilize the micelles efficiently.

5. Conclusions

The effect of a series of cations on the rheological properties of 300 mM SLES+CAPB 2:1 surfactant mixture is studied and compared to the solutions of SLES alone. The experiments reveal that the ions with higher Z/R ratio (smaller hydrated radius at similar valence, or higher valence at similar hydrate ion radius) are more efficient in the formation of wormlike micelles. This is due to their stronger electrostatic

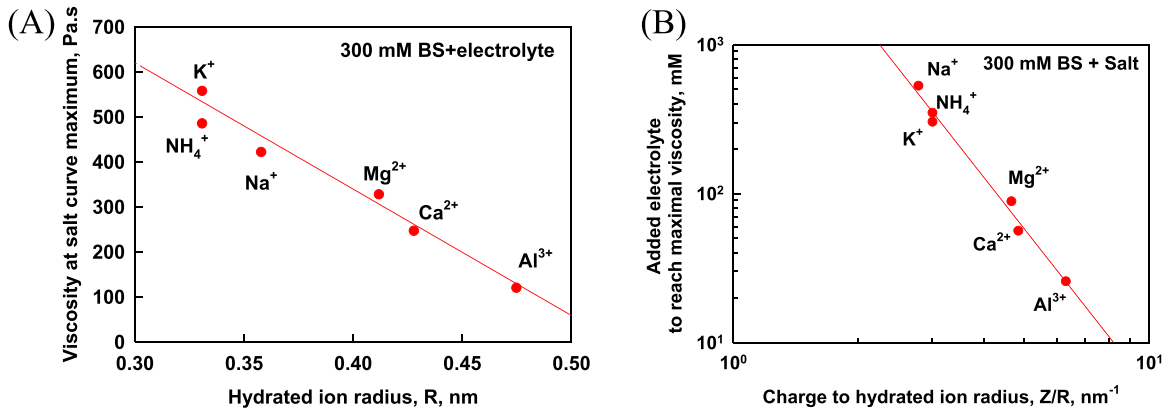

Fig. 6. (A) Viscosity as a function of hydrated ion radius and (B) added electrolyte concentration in viscosity maximum as a function of counter ion to surfactant ratio.

interaction with the oppositely charged sulfate (in SLES) and carboxylate (in CAPB) headgroups in the mixture studied. In addition, highly hydrated cations lead to lower maximum in the viscosity (probably via a switch from entangled to branched micelles), accompanied by faster relaxation, breakage and reptation of the micelles.

We observed a qualitative difference in the effect of counterions on the SLES and on SLES+CAPB surfactant solutions. The viscosity of the mixed SLES+CAPB solution is by ten times higher when compared to the single SLES, due to the hindrance of the electrostatic repulsion between the SLES headgroups by the zwitterionic CAPB component. For SLES+CAPB system, the viscosity peak is higher for K^+ compared to Na^+, whereas the opposite trend is observed for SLES. The viscosity peak for Ca^{2+} is also higher as compared to Mg^{2+} and the magnitude of the viscosity peak for SLES+CAPB system decreases with increasing the size of the hydrated ions. The complex interactions of the counterions with both surfactant components are important for the length of the wormlike micelles and for the micelle branching, while the peak position (driven by the process of micelle elongation) is not significantly affected by the presence of CAPB in the SLES+CAPB mixture.

All experimental results are explained mechanistically by considering both the strength of the counterion interactions and the specific arrangement of the counterions on the micelle surface which affect the bending stiffness and, hence, the transition from entangled into branched micelles, see Fig. 5. The proposed explanations complement the previous studies in this area and advance them into the rich realm of surfactant mixtures which is increasingly attracting attention from both fundamental and application viewpoints.

CRediT authorship contribution statement

Zlatina Mitrinova: Investigation, Formal analysis, Visualization, Writing – original draft. **Hristo Alexandrov:** Investigation, Formal analysis. **Nikolai Denkov:** Conceptualization, Methodology, Writing – review & editing. **Slavka Tcholakova:** Conceptualization, Methodology, Formal analysis, Writing – review & editing, Supervision.

Declaration of Competing Interest

The authors declare that they have no known competing financial interests or personal relationships that could have appeared to influence the work reported in this paper.

Acknowledgements

Zlatina Mitrinova acknowledges the financial support received from the program “Young scientists and Postdoctoral candidates" of the Bulgarian Ministry of Education and Science, MCD № 577/17.08.2018. This work was partially supported by Operational Program ”Science and Education for Smart Growth” 2014–2020, co-financed by European Union through the European Structural and Investment Funds, Grant BG05M2OP001-1.002-0012 “Sustainable Utilization of Bio-resources and Waste of Medicinal and Aromatic Plants for Innovative Bioactive Products”. The authors are grateful to the reviewers for their very useful comments and suggestions.

Appendix A. Supporting information

Supplementary data associated with this article can be found in the online version at doi:10.1016/j.colsurfa.2022.128746.

References

[1] M. Pleines, W. Kunz, T. Zemb, D. Benczedi, W. Fieber, Molecular factors governing the viscosity peak of giant micelles in the presence of salt and fragrances, J. Colloid Interface Sci. 537 (2019) 682–693.
[2] Israelachvili, J., Intermolecular and Surface Forces, third ed., Academic Press, 2011.
[3] C.A. Herb, R.K. Prud’homme, (Eds.), Structure and Flow of Surfactant Solutions, Symp.Ser. 578, ACS, Washington, 1994.
[4] K. Aramaki, S. Hoshida, S. Arima, Effect of carbon chain length of cosurfactant on the rheological properties of nonionic wormlike micellar solutions formed by a sugar surfactant and monohydroxy alcohols, Colloids Surf. A 366 (2010) 58–62.
[5] K. Aramaki, S. Hoshida, S. Arima, Formation of wormlike micelles with natural-sourced ingredients (sucrose fatty acid ester and fatty acid) and a viscosity-boosting effect induced by fatty acid soap, Colloids Surf. A 396 (2012) 278.
[6] S.R. Raghavan, G. Fritz, E.W. Kaler, Wormlike micelles formed by synergistic self-assembly in mixtures of anionic and cationic surfactants, Langmuir 18 (2002) 3797.
[7] C. Oelschlaeger, N. Willenbacher, Mixed wormlike micelles of cationic surfactants: effect of the cosurfactant chain length on the bending elasticity and rheological properties, Colloids Surf. A 406 (2012) 31–37.
[8] Z. Mitrinova, S. Tcholakova, N. Denkov, Control of surfactant solution rheology using medium-chain cosurfactants, Colloids Surf. A Physicochem. Eng. Asp. 537 (2018) 173–184.
[9] D.P. Acharya, H. Kunieda, Wormlike micelles in mixed surfactant solutions, Adv. Colloid Interface Sci. 123–126 (2006) 401–413.
[10] L. Ziserman, L. Abezgauz, O. Ramon, S.R. Raghavan, D. Danino, Origins of the viscosity peak in wormlike micellar solutions. 1. Mixed catanionic surfactants. A cryo-transmission electron microscopy study, Langmuir 25 (18) (2009) 10483–10489.
[11] D. Acharya, T. Sato, M. Kaneko, Y. Singh, H. Kunieda, Effect of added poly (oxyethylene)dodecyl ether on the phase and rheological behavior of wormlike micelles in aqueous SDS solutions, J. Phys. Chem. B 110 (2) (2006) 754–760.
[12] R.A. Abdel-Rahem, M. Reger, M. Hloucha, H. Hoffmann, Rheology of aqueous solutions containing SLES, CAPB, and microemulsion: influence of cosurfactant and salt, J. Dispers. Sci. Technol. 35 (2014) 64–75.
[13] A. Parker, W. Fieber, Viscoelasticity of anionic wormlike micelles: effects of ionic strength and small hydrophobic molecules, Soft Matter 9 (2013) 1203–1213.
[14] G.S. Georgieva, S.E. Anachkov, I. Lieberwirth, K. Koynov, P.A. Kralchevsky, Synergistic growth of giant wormlike micelles in ternary mixed surfactant solutions: effect of octanoic acid, Langmuir 32 (2016) 12885–12893.
[15] S.E. Anachkov, G.S. Georgieva, L. Abezgauz, D. Danino, P.A. Kralchevsky, Viscosity peak due to shape transition from wormlike to disklike micelles: effect of dodecanoic acid, Langmuir 34 (2018) 4897–4907.

[16] Y. Qiao, Y. Lin, Y. Wang, Z. Li, J. Huang, Metal-driven viscoelastic wormlike micelle in anionic/zwitterionic surfactant systems and template-directed synthesis of dendritic silver nanostructures, Langmuir 27 (5) (2011) 1718–1723.
[17] X. Tang, W. Zou, P. Koenig, S. McConaughy, M. Weaver, D. Eike, M. Schmidt, R. Larson, Multiscale modeling of the effects of salt and perfume raw materials on the rheological properties of commercial threadlike micellar solutions, J. Phys. Chem. B 121 (2017) 2468–2485.
[18] L. Abezgauz, K. Kuperkar, P.A. Hassan, O. Ramon, P. Bahadur, D. Danino, Effect of Hofmeister anions on micellization and micellar growth of the surfactant cetylpyridinium chloride, J. Colloid Interface Sci. 342 (2010) 83–92.
[19] C. Oelschlaeger, P. Suwita, N. Willenbacher, Effect of counterion binding efficiency on structure and dynamics of wormlike micelles, Langmuir 26 (10) (2010) 7045–7053.
[20] F. Hofmeister, Zur Lehre von der Wirkung der Salze, Arch. Exp. Pathol. Pharmakol. 27 (1890) 395–413.
[21] F.Zur Hofmeister, Lehre von der Wirkung der Salze, Arch. Exp. Pathol. Pharmakol. 28 (1891) 210–238.
[22] K.D. Collins, G.W. Neilson, J.W. Enderby, Ions in water: characterizing the forces that control chemical processes and biological structure, Biophys. Chem. 128 (2007) 95–104.
[23] N. Vlachy, B. Jagoda-Cwiklik, R. Vácha, D. Touraud, P. Jungwirth, W. Kunz, Hofmeister series and specific interactions of charged headgroups with aqueous ions, Adv. Colloid Interface Sci. 146 (2009) 42–47.
[24] Z.H. Ren, Mechanism of the salt effect on micellization of an aminosulfonate amphoteric surfactant, Ind. Eng. Chem. Res. 54 (2015) 9683–9688.
[25] E. Dutkiewicz, A. Jakubowska, Effect of electrolytes on the physicochemical behaviour of sodium dodecyl sulphate micelles, Colloid Polym. Sci. 280 (2002) 1009–1014.
[26] K.K. Sharker, Md.N. Islam, D. Shuvo, Interactions of some Hofmeister cations with sodium dodecyl sulfate in aqueous solution, J. Surfactant Deterg. (2018).
[27] R. Alargova, J. Petkov, D. Petsev, I.B. Ivanov, G. Broze, A. Mehreteab, Light scattering study of sodium dodecyl polyoxyethylene-2 sulfate micelles in the presence of multivalent counterions, Langmuir 11 (1995) 1530–1536.
[28] R.G. Alargova, K.D. Danov, J.T. Petkov, G. Broze, Sphere-to-rod transition in the shape of anionic surfactant micelles determined by surface tension measurements, Langmuir 13 (1997) 5544–5551.
[29] R.G. Alargova, K.D. Danov, P.A. Kralchevsky, G. Broze, A. Mehreteab, Growth of giant rodlike micelles of ionic surfactant in the presence of Al^{3+} counterions, Langmuir 14 (1998) 4036–4049.
[30] R. Alargova, I.B. Ivanov, P.A. Kralchevsky, A. Mahreteab, G. Broze, Growth of rod-like micelles in anionic surfactant solutions in the presence of Ca^{2+} counterions, Colloids Surf. A Physicochem. Eng. Asp. 142 (1998) 201–218.
[31] H. Xu, J. Penfold, R.K. Thomas, J.T. Petkov, I. Tucker, J.R.P. Webster, I. Grillo, A. Terry, Ion specific effects in trivalent counterion induced surface and solution self-assembly of the anionic surfactant sodium polyethylene glycol monododecyl ether sulfate, Langmuir 30 (2014) 4694–4702.
[32] M.I. Alkschbirsa, A.M. Perceboma, W. Loha, H. Westfahl Jr., M.B. Cardosob, E. Sabadinia, Effects of some anions of the Hofmeister series on the rheology ofcetyltrimethylammonium-salicylate wormlike micelles, Colloids Surf. A Physicochem. Eng. Asp. 470 (2015) 1–7.
[33] Y. Marcus, Thermodynamics of solvation of ions part 5.4ibbs free energy of hydration at 298.15 K, J. Chem. Soc. Faraday Trans. 87 (18) (1991) 2995–2999.
[34] A.G. Zilman, S.A. Safran, Role of cross-links in bundle formation, phase separation and gelation of long filaments, Europhys. Lett. 63 (2003) 139.
[35] N.A. Spenley, M.E. Cates, T.C.B. McLeish, Nonlinear rheology of wormlike micelles, Phys. Rev. Lett. 71 (1993) 939.
[36] Z. Mitrinova, S. Tcholakova, Z. Popova, N. Denkov, B.R. Dasgupta, K. P. Ananthapadmanabhan, Efficient control of the rheological and surface properties of surfactant solutions containing C8−C18 fatty acids as cosurfactants, Langmuir 29 (2013) 8255–8265.
[37] Z. Chu, Y. Feng, X. Su, Y. Han, Wormlike micelles and solution properties of a C22-tailed amidosulfobetaine surfactant, Langmuir 26 (11) (2010) 7783–7791.
[38] N.C. Christov, N.D. Denkov, P.A. Kralchevsky, K.P. Ananthapadmanabhan, A. Lips, Synergistic sphere-to-rod micelle transition in mixed solutions of sodium dodecyl sulfate and cocoamidopropyl betaine, Langmuir 20 (2004) 565–571.
[39] S.J. Candau, A. Khatory, F. Lequeux, F. Kern, Rheological behaviour of wormlike micelles: effect of salt content, J. Phys. IV 3 (1993) 197.
[40] A. Khatory, F. Lequeux, F. Kern, S.J. Candau, Linear and nonlinear viscoelasticity of semidilute solutions of wormlike micelles at high salt content, Langmuir 9 (1993) 1456–1464.
[41] P.J. Missel, N.A. Mazer, M.C. Carey, G. BenedekInfluence B., Influenceof alkali-metal counterion identity on the sphere-to-rod transition in alkyl sulfate micelles, J. Phys. Chem. 93 (1989) 8354–8366.
[42] H. Xu, J. Penfold, R.K. Thomas, J.T. Petkov, I.M. Tucker, I. Grillo, A. Terry, Impact of AlCl3 on the self-assembly of the anionic surfactant sodium polyethylene glycol monoalkyl ether sulfate in aqueous solution, Langmuir 29 (2013) 13359–13366.
[43] Z. Mitrinova, S. Tcholakova, K. Golemanov, N. Denkov, M. Vethamuthu, K. P. Ananthapadmanabhan, Surface and foam properties of SLES + CAPB + fatty acid mixtures: effect of pH for C12–C16 acids, Colloids Surf. A Physicochem. Eng. Asp. 438 (2013) 186–198.
[44] V. Lutz-Bueno, M. Liebi, J. Kohlbrecher, P. Fischer, Intermicellar interactions and the viscoelasticity of surfactant solutions: complementary use of SANS and SAXS, Langmuir 33 (10) (2017) 2617–2627.
[45] E.A. Kelly, N. Willis-Fox, J.E. Houston, C. Blayo, G. Divitini, N. Cowieson, R. Daly, R.C. Evans, A single-component photorheological fluid withlight-responsive viscosity, Nanoscale 12 (2020) 6300–6306.
[46] L.A. Fielding, J.A. Lane, M.J. Derry, O.O. Mykhaylyk, S.P. Armes, Thermo-responsive diblock copolymer worm gels in non-polar solvents, J. Am. Chem. Soc. 136 (2014) 5790–5798.
[47] O. Glatter, O. Kratky, Small-angle X-ray Scattering, Academic Press, London, 1982.
[48] J. Wang, Y. Feng, N.R. Agrawald, S.R. Raghavan, Wormlike micelles versus water-soluble polymers as rheology-modifiers: similarities and differences, Phys. Chem. Chem. Phys. 19 (2017) 24458.
[49] K. Eguchi, I. Kaneda, Y. Hiwatari, H. Masunaga, K. Sakuraia, Salt-concentration dependence of the structure and form factors for the wormlike micelle made from a dual surfactant in aqueous solutions, J. Appl. Cryst. 40 (2007) s264–s268.
[50] K. Naruse, K. Eguchi, I. Akiba, K. Sakurai, H. Masunaga, H. Ogawa, J.S. Fossey, Flexibility and cross-sectional structure of an anionic dual-surfactant wormlike micelle explored with small-angle X-ray scattering coupled with contrast variation technique, J. Phys. Chem. B 113 (2009) 10222–10229.
[51] J. Lipfert, L. Columbus, X. Vincent, B. Chu, S.A. Lesley, S. Doniach, Size and shape of detergent micelles determined by small-angle X-ray scattering, J. Phys. Chem. B 111 (2007) 12427–12438.
[52] J.J. Cardiel, Y. Zhao, P. De La Iglesia, L.D. Pozzocand, A.,Q. Shen, Turning up the heat on wormlike micelles with a hydrotopic salt in microfluidics, Soft Matter 10 (2014) 9300.
[53] V.M. Garamus, J.S. Pedersen, H. Kawasaki, H. Maeda, Scattering from polymerlike micelles of TDAO in salt/water solutions at semidilute concentrations, Langmuir 16 (2000) 6431–6437.
[54] V.T. Kelleppan, J.E. Moore, T.M. McCoy, A.V. Sokolova, L. de Campo, B. L. Wilkinson, R.F. Tabor, Self-assembly of long-chain betaine surfactants: effect of tailgroup structure on wormlike micelle formation, Langmuir 34 (3) (2018) 970–977.
[55] M.E. Cates, Reptation of living polymers: dynamics of entangled polymers in the presence of reversible chain-scission reactions, Macromolecules 20 (9) (1987) 2289–2296.
[56] Vrbka, l , Vondrášek, J. , Jagoda-Cwiklik, B. , Vácha, R. , Jungwirth, P. Quantification and rationalization of the higher affinity of sodium over potassium to protein surfaces, PNAS, October 17, 2006 103 (42) 15440–15444. doi: 10.1073/pnas.0606959103.
[57] A. Salis, B.W. Ninham, Models and mechanisms of Hofmeister effects in electrolyte solutions, and colloid and protein systems revisited, Chem. Soc. Rev. 43 (2014) 7358.